ZÁPADOČESKÁ UNIVERZITA V PLZNI

FAKULTA STROJNÍ

KATEDRA ENERGETICKÝCH STROJŮ A ZAŘÍZENÍ

ZÁPADOČESKÁ UNIVERZITA V PLZNI

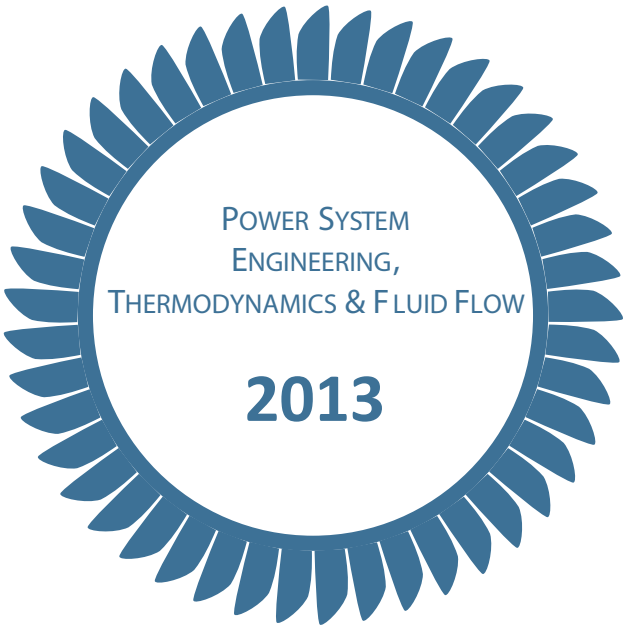

JEDNOTLIVÝ PŘÍSPĚVEK ZE SBORNÍKU

evropský sociální fond v ČR
EVROPSKÁ UNIE
MINISTERSTVO ŠKOLSTVÍ, MLÁDEŽE A TĚLOVÝCHOVY
OP Vzdělávání pro konkurenceschopnost
INVESTICE DO ROZVOJE VZDĚLÁVÁNÍ

ELABORATION OF THE FLOW SYSTEM FOR A COGENERATION ORC TURBINE

RUSANOV Andrey, LAMPART Piotr, RUSANOV Roman, BYKUC Sebastian

The paper describes methods of design of several variants of blading systems for axial and radial-axial flow turbines for a 100 kW Organic Rankine Cycle (ORC) cogeneration unit. The radial-axial turbine has a slightly lower aerodynamic efficiency than the axial turbine, however it consists only of a single stage as compared to the multi-stage axial turbine design.

Keywords: cogeneration unit, Organic Ranking Cycle, CFD, axial turbine, radial-axial turbine

Introduction

A promising technology for small scale cogeneration systems is Organic Rankine Cycle (ORC) [1]. Main components of this cogeneration cycle are a heat source, eg. ecological boiler fit to combust different kinds of biomass or biofuels, intermediate heat cycle to extract heat from flue gases to thermal oil as a heat carrier, and the main cycle including the evaporator, turbine driving a generator, recuperator, condenser and circulating pumps for the working medium and thermal oil. Depending on the available heat source and particular application there are variety of working media that can be used for ORC. The solution offers a possibility to apply low temperature heat sources, allows utilisation of different types of fuels, and also a modular construction which facilitates adaptation of the CHP unit to the required power range. One can think of micro CHP units dedicated for individual households of total heat capacity up to 20kWt and electric power up to 4kWe as well as small CHP modules dedicated for communal energy centres of total heat capacity 500kWt and electric power 100kWe (maximum up to 5 MWt and 1 MWe, respectively).

1. Scheme of the cycle. Input data for turbine design

A scheme of the ORC cycle with the silica oil MDM as a working medium for the electric power just below 100 kW is presented in Fig. 1. The following input data for the turbine design are assumed: mass flow rate – 1,51 kg/s; inlet pressure 12 bar, inlet temperature 553 K, exit pressure 0.17 bar, rotational speed – 3000 or 9000 rev/min (for the axial turbine) and up to 16000 rev/min (for the radial-axial turbine). The following geometric restrictions are assumed for the axial turbine flow system: minimum blade height - 15 mm, maximum axial length 800 mm, maximum stage number – 9 (for 9000 rev/min), 14 (for 3000 rev/min); for the radial-axial turbine flow system: minimum blade height – basically 10 mm, however blade heights of 5 mm are also considered, maximum stage number – 1.

2. Method for design and gasdynamic evaluation of the turbine flow system

The design of the turbine flow system consists of several elements: computation of basic geometric and flow characteristics using 1D methods, building 3D geometry of the flow path, 3D calculations and optimisation.

Computation of basic geometric and flow characteristics.

This is made with the help of 1D equations of conservation of mass and rotalpy, appropriate treatment of velocity triangles and correlations for kinetic energy losses [2].

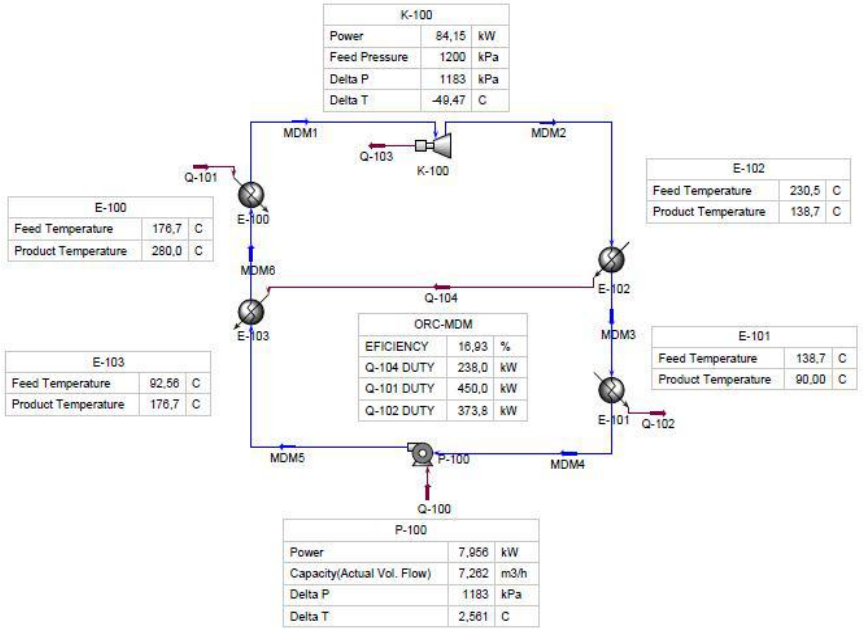

Fig. 1: Scheme of the cogeneration ORC cycle (working medium – silica oil MDM)

The search for the optimum geometric characteristics proceeds from a great number of variants taking into account the assumed flow and constructional restrictions:

- properties of the working medium (incorporated in the form of the Tammann equation), inlet/exit parameters;
- stage reactions (minimum and maximum values), blade heights (minimum and maximum values), stator exit angles (minimum and maximum values), rotor inlet angles in the relative frame (minimum and maximum values), rotor exit angles in the absolute frame (minimum and maximum values), maximum stator and rotor exit Mach numbers;
- mid-span radiuses at rotor inlet/exit (minimum and maximum values), stator and rotor throat areas (minimum and maximum values), rotational speed (minimum and maximum values).

As a result of computations, geometric and gasdynamic characteristics are obtained referring to the maximum possible turbine power: flow angles and velocities in absolute and relative frame, mid-span radiuses, blade heights, mean values of thermodynamic parameters, rotational speed and turbine power.

Building 3D geometry of the flow system

This is made by means of parametrisation and analythical profiling of the blading system [3]. The blades are defined by plane profiles (Fig. 2) described by leading and trailing edges, suction and pressure curves. The leading and trailing edges are circle arcs. The suction and pressure curves are polynomials of the 5-th and 4-th order, respectively:

$$y(x)=\sum_{i=0}^{5} a_i x^i \ , \ a_i = const \qquad (1)$$

$$y(x)=\sum_{i=0}^{4} a_i x^i \ , \ a_i = const \qquad (2)$$

The input data for building the profile cascade are: b_x – profile width, α_1 – camber line inlet angle; r_1 – leading edge radius; α_{2ef} – cascade effective angle; r_2 – trailing edge radius, t – cascade pitch; α_{2s} – geometric angle; $\Delta\alpha_1$, $\Delta\alpha_2$ – leading and trailing edge angles.

Coefficients of the suction curve (1) are found from the following set of equations:

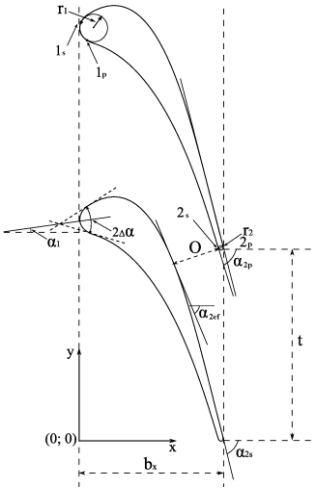

Fig. 2: Cascade of profiles

$$\begin{cases} y_s'(x_{1s}) = tg(\alpha_1 + \Delta\alpha_1) \\ y_s''(x_{1s}) = \{y_{s,0}''\} \\ y_s(x_O) = y_O \\ y_s'(x_O) = tg(\alpha_o) \\ y_s(x_{2s}) = y_{2s} \\ y_s'(x_{2s}) = tg\{\alpha_{2s}\} \end{cases}; \tag{3}$$

where x_{1s}, y_{1s}, x_{2s}, y_{2s} are coordinates of the tangency points with the leading/trailing edge circles, α_{2s} and y_0'' are varying parameters chosen in a way to provide the assumed value of throat O and assure the minimum curvature. The throat can be calculated from the cascade pitch and effective angle

$$O = t\cos\alpha_{2ef}.$$

After the determination of the suction surface as well as leading and trailing edges, coefficients of the pressure curve (2) are found from the following set of equations:

$$\begin{cases} y_p(x_{1p}) = y_{1p} \\ y_p'(x_{1p}) = tg(\alpha_1 - \Delta\alpha) \\ y_p''(x_{1p}) = \{y_{p,0}''\} \\ y_p(x_{2p}) = y_{2p} \\ y_p'(x_{2p}) = tg\alpha_{2p} \end{cases}; \tag{4}$$

where x_{1p}, y_{1p}, x_{2p}, y_{2p} are coordinates of the tangency points with the leading/trailing edge circles, which can be found from the assumed angle α_1-$\Delta\alpha$ at the leading edge and angle α_{2p} at the trailing edge. The angle α_{2p} is found from the range between α_{2ef} and α_{2s} so as to assure the minimum curvature of the pressure curve.

In order to reduce the number of free parameters, initial data are given in three cross-sections. The cascade pitch is evaluated from the cross-section radius and blade number. Building a profile in any sections is based on quadratic approximations assuring a monotonous change of the profile surface.

For building the radial-axial turbine stage, a method described in [4] is used (Fig. 3). The leading edge is assumed parallel to the rotational axis x, the trailing edge is normal.

Tip and hub endwalls are described by arc circles and straight intervals. The initial data for

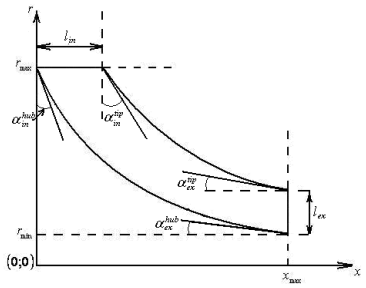

Fig. 3: View of the rotor in meridional plane

building endwall curves are: $r_{\max}$, $r_{\min}$ − maximum and minimum radiuses of the rotor channel; $x_{\max}$ − rotor width; l_{in}, l_{ex} − inlet and exit heights; α_{in}^{hub}, α_{ex}^{hub}, α_{in}^{tip}, α_{ex}^{tip} − angles of the tip and hub endwalls at the inlet and exit (Fig. 3).

The blade is defined on two sections of rotational surfaces of the tip and hub endwalls. The sections are described by coordinates: $r\varphi$ − along the circumference; s − distance from the leading edge. Profile coordinates on rotational surfaces of the tip and hub endwalls are found as a sum of coordinates for the mean line $r\varphi_{ml}$ (Fig. 4a) and profile thickness $\Delta r\varphi$ (Fig. 4b):

$$r\varphi(s) = r\varphi_{ml}(s) + \Delta r\varphi(s).$$

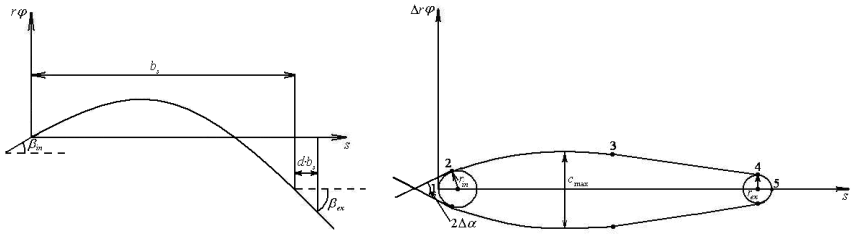

a) b)

Fig. 4: Blade section: a − blade mean line; b − blade thickness with respect to the mean line

The mean line is a 3-rd order polynomial (Fig. 4a):

$$r\varphi_{ml} = \sum_{i=0}^{3} a_i s^i ,$$

where a_i − coefficients. The profile, symmetrical with respect to the mean line is composed of: 1-2 − leading edge; 2-3 − arc circle; 3-4 − straight interval; 4-5 − trailing edge.

The initial data for building the profile are: b_s − profile width; β_{in}, β_{ex} − mean line angles at the leading and trailing edge; r_{in}, r_{ex} − leading/trailing edge radiuses; c_{max} − maximum profile thickness; $\Delta\alpha$ − leading edge angle; d − distance from the trailing edge, where the second derivative of the mean line equals 0 (Fig. 4).

Method for solving 3D flow

Flow computations are made with the help of a code ***FlowER*** [5, 6], which draws on the following mathematical models: Reynolds (Favre) averaging of Navier-Stokes equations, SST turbulence model of Menter, implicit quasi-monotonous high-order ENO scheme. The results of computations obtained from the code ***FlowER*** provide flow details and global characteristics of turbine blading systems [7, 8].

3. Axial turbines for 3000 and 9000 rev/min

Two variants of axial turbines for 3000 and 9000 rev/min are considered. The meridional section of turbine 1 (for 3000 rev/min) is presented in Fig. 5, whereas turbine geometric characteristics are gathered in Table 1.

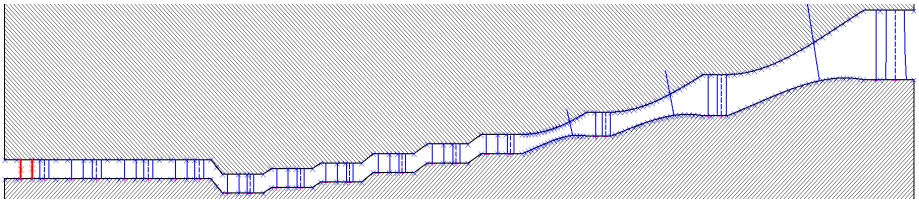

Fig. 5: Meridional section of turbine 1

Table 1

Geometric characteristics of blading system for turbine 1

Stage number	**1**	**2**	**3**	**4**	**5**	**6**	**7**
Partial admission	0,2	0,2	0,25	0,5	1	1	1
α_0, deg	0	-60	-60	-60	-60	-60	-60
α_1, deg	78	74,64	72,40	77,44	77	77	77
β_1, deg	71,52	68,883	66,474	72,7741	69,6915	70,0585	70,789
β_2, deg	-72,68	-69,88	-67,64	-73,8	-72,95	-72,95	-72,41
α_2, deg	-57,9	-60,171	-58,38282	-65,8285	-59,141	-59,98	-59,885
r_{mid}, mm	76,1	76,1	76,1	76,1	64,8	69,11	73,48
l, mm	15,0256	15,1975	15,13532	15,26	15,06	15,01	15,027
Stage number	**8**	**9**	**10**	**11**	**12**	**13**	
Partial admission	1	1	1	1	1	1	
α_0, deg	-60	-60	-60	60	60	60	
α_1, deg	76,73	75,92	74,03	73,26	75,13	77	
β_1, deg	70,43665	69,688	68,25	67,94	69,275	64,64685	
β_2, deg	-72,14	-71,33	-69,17	-68,075	-69,52	-67,82	
α_2, deg	-59,801	-59,877	-59,392	-59,49	-59,07	-18,7156	
r_{mid}, mm	81	88,6	96,2	112	135	175	
l, mm	15,101	15,103	15,259	19,006	32,745	55,2878	

The flow path consists of 13 stages, out of which the first four stages have a partial admission to fulfil the requirement of a minimum blade height of 15 mm. The first ten stages have cylindrical blades. The last three stages have a largely increasing diameter. The endwalls have 3D contours there, stator blades are twisted with wide chords, the last rotor blades are 3D shaped (Fig. 6). Owing to that the flow has regular patterns (Fig. 7, 8).

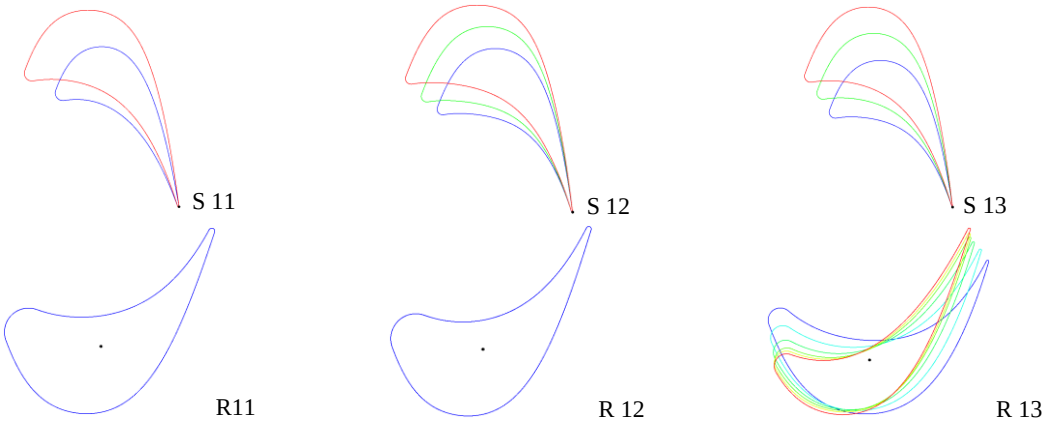

Fig. 6: Hub-to-tip sections of stator and rotor blades for stages 11-13

Due to the assumed stage number and turbine length restrictions, the blades operate as highly loaded with the velocity coeffecients u/c equal about 0.25 and high turning angles. The stage exit swirl angles are near 60 deg. The turbine efficiency is equal to 76%, turbine power - 76,8 kW. The obtained efficiency level seems to be satisfactory. However , in order to increase it is necessary to increase the velocity coefficients u/c which can be done by increasing the number of stages up to eg. 20 or by increasing the rotational speed of the rotor.

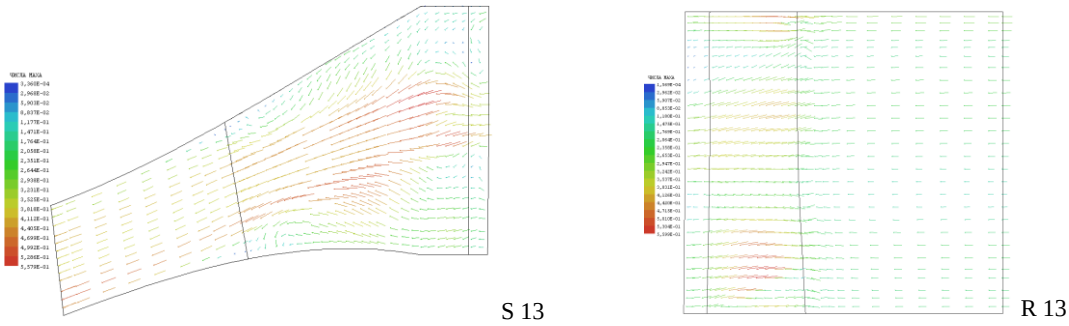

Fig. 7: Velocity vectors coloured by Mach number at mid blade-to-blade distance of stage 13

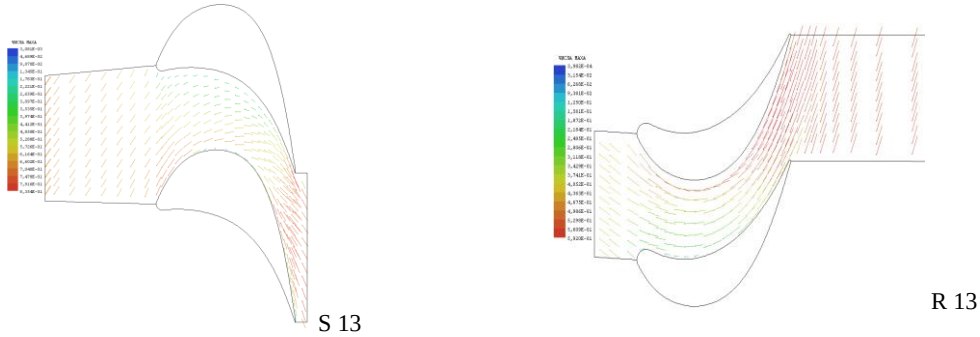

Fig. 8: Velocity vectors coloured by Mach number at mid span of stage 13

The meridional section of turbine 2 (for 9000 rev/min) is presented in Fig. 9, whereas turbine geometric characteristics are collected in Table 2. This variant consists of 7 stages. The first three stages have a partial admission. The last three stages have 3D shaped blades (Fig. 10), endwall contours are also 3D shaped there. The blade loading is optimal as compared with the turbine variant for 3000 rev/min, with the velocity coefficients u/c on the level of 0.45. The stage exit swirl angles are near 0. The obtained velocity vectors are regular (Fig. 11, 12). The flow efficiency of the turbine for 9000 rev/min is considerably higher than for 3000 rev/min and is equal to 84,2 %.

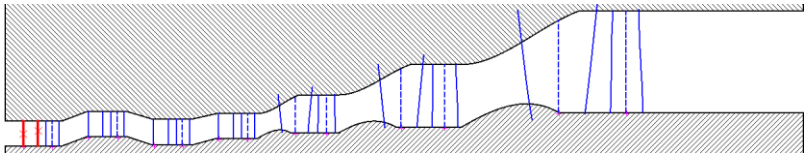

Fig. 9: Meridional section of turbine 2

Table 2

Geometric characteristics of blading system for turbine 2

Stage number	**1**	**2**	**3**	**4**	**5**	**6**	**7**
Partial admission	0,25	0,4	0,75	1	1	1	1
α_0, deg	0	0	0	0	0	0	0
α_1, deg	77,72	78	78	77	77	77	77
β_1, deg	61,64875	64,77799	63,319066	63,56912	63,7599	62,15225	49,8569
β_2, deg	-65,52	-67,86	-67,86	-67,86	-67,08	-65,52	-66,3
α_2, deg	15,5785	-3,317	7,18631	-17,691	-13,43267	3,485	7,4917
r_{mid}, mm	58	63,61	58,92	62,6	70	80,9	101,68
l, mm	15,283	15,3	15,7958	15,1035	23,08715	38,21	62,0338

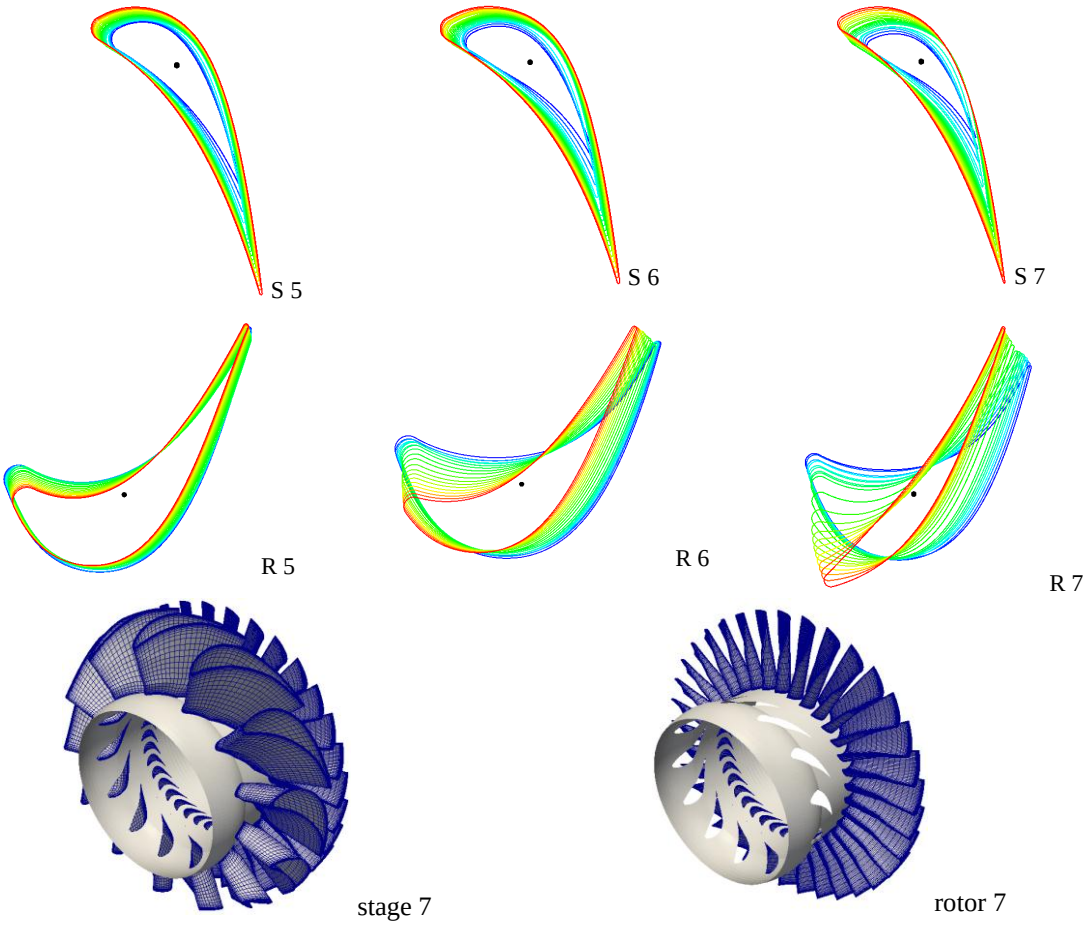

Fig. 10: Hub-to-tip sections of stator and rotor blades for stages 5-7 and isometric view of stage 7

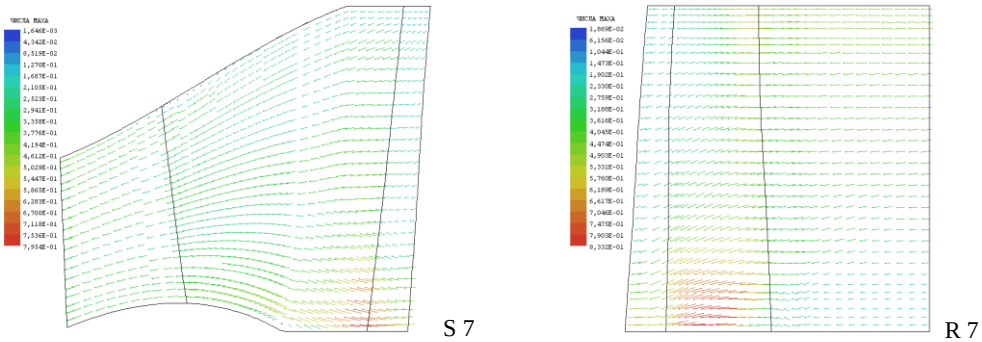

Fig. 11: Velocity vectors coloured by Mach number at mid blade-to-blade distance of stage 7

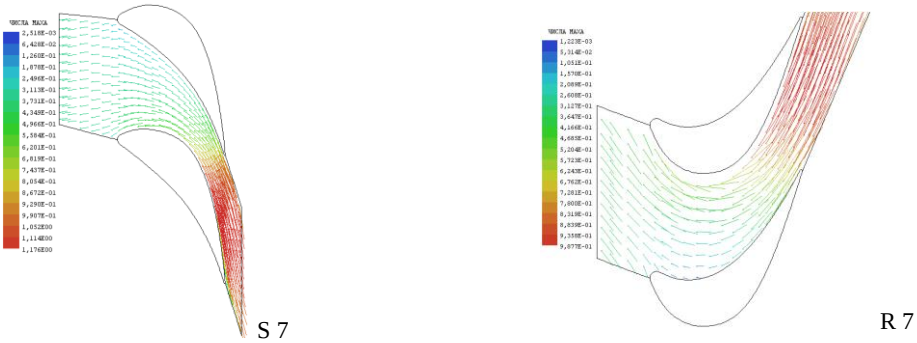

Fig. 12: Velocity vectors coloured by Mach number at mid span of stage 7

4. Radial-axial turbines

Three variants of radial-axial turbines are considered here whose geometric characteristics of the stator-rotor flow system are shown in consecutive Tables 3, 4, 5.

A view of the flow system for radial-axial turbine, variant 1 is presented in Fig. 13. The rotor rotational speed is equal to 14000 rev/min.

Table 3

Geometric characteristics of flow path for radial-axial turbine – variant 1

r_{in}, S	r_{ex}, S	l_{in}, S	l_{ex}, S	z, S
232,96	199	5,43	5,43	57
r_{in}, R	$r_{mid.ex}$, R	l_{in}, R	l_{ex}, R	z, R
185	85,105	5,43	70.19	11

Table 4

Geometric characteristics of flow path for radial-axial turbine – variant 2

r_{in}, S	r_{ex}, S	l_{in}, S	l_{ex}, S	z, S
215.38	181	10.36	10.36	57
r_{in}, R	$r_{mid.ex}$, R	l_{in}, R	l_{ex}, R	z, R
167.75	115.59	10.36	55.96	17

Table 5

Geometric characteristics of flow path for radial-axial turbine – variant 3

r_{in}, S	r_{ex}, S	l_{in}, S	l_{ex}, S	z, S
215,35	181	5,18	5,18	57
r_{in}, R	$r_{mid.ex}$, R	l_{in}, R	l_{ex}, R	z, R
168,75	115,59	5,18	27,98	17

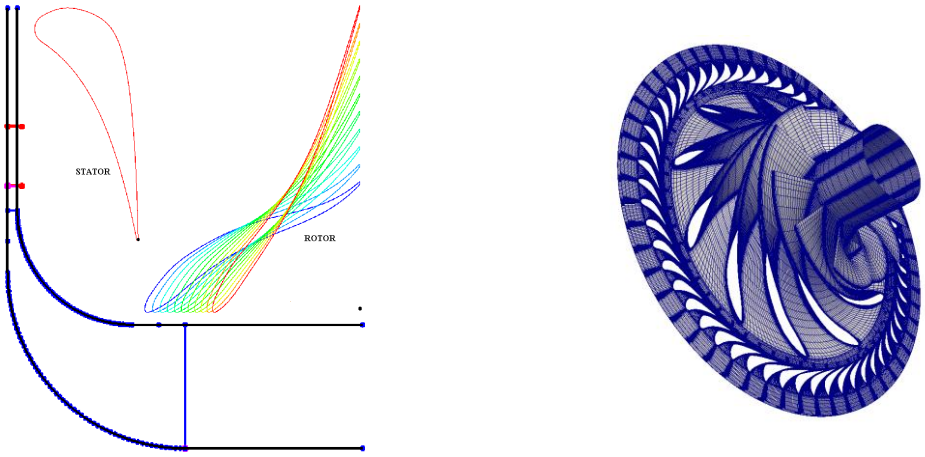

Meridional section Isometric view

Fig. 13: View of the flow system for radial-axial turbine – variant 1

Although the flow system consists of only one stage which consumes a large pressure drop, flow pictures look favourable for this variant (Fig. 14-17). The maximum Mach number in the entire flow domain does not exceed 2. The flow patterns do not exhibit shock phenomena nor separations. As a result, the flow efficiency is high and equals 88,5 % (tip leakage not considered). On the other hand, the minimum blade height at the inlet to the above radial-axial turbine variant is low and equal to 5.43 mm, which can be a cause of technological difficulties. Therefore, variant 2 was also elaborated where the minimum blade height at the inlet is 10.36 mm and the rotational speed amounts to 12000 rev/min. The flow efficiency of this variant is slightly lower than for variant 1 but it is still high - 79,9 %.

The obtained radial-axial turbines are characterised by a high reaction contrary to the previously considered impulse-type axial turbines. Thus, another variant 3 of the two-stage radial-axial turbine for 12000 rev/min was elaborated where the radial inflow is divided into

two symmetrical streams moving in opposite directions. In this variant the flow efficiency was also found to be relatively high and equal to 78 %.

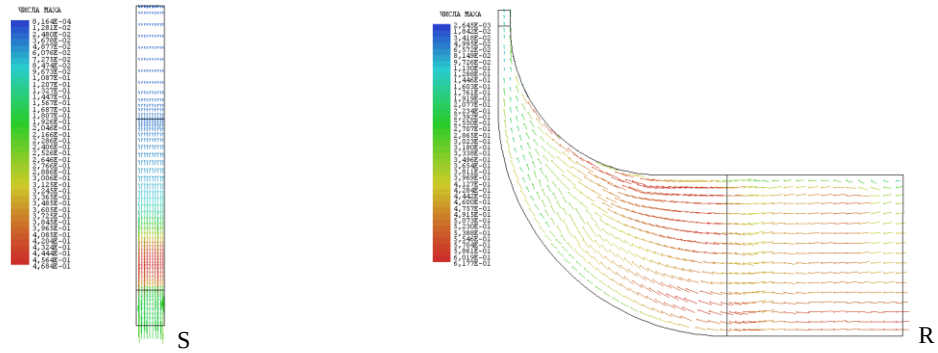

Fig. 14: Velocity vectors coloured by Mach number at mid blade-to-blade section

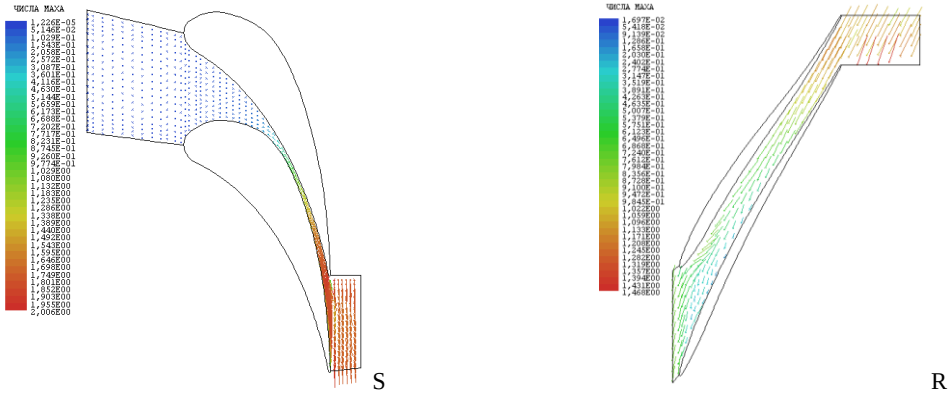

Fig. 15: Velocity vectors coloured by Mach number at mid blade span

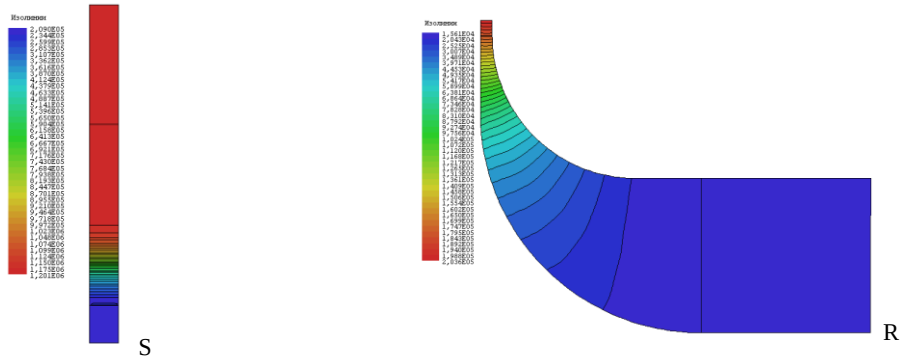

Fig. 16: Static pressure contours at mid blade-to-blade section

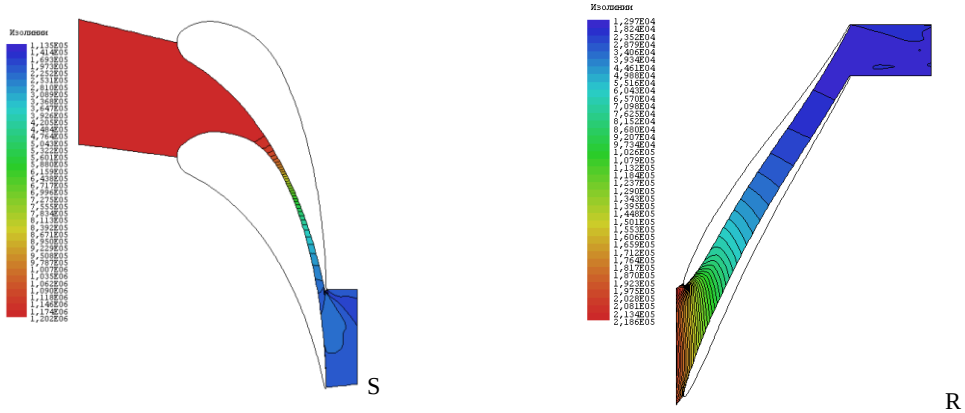

Fig. 17:. Static pressure contours at mid blade span

Conclusions

The described design method enables the elaboration of axial and radial-axial turbines for ORC cogeneration units. Several variants of the flow path of axial and radial-axial turbines of power just below 100 kW were presented. All turbine variants exhibit satisfactory flow efficiencies. Due to the assumed constructional restrictions, turbine rotors with a higher rotational speed are more effective. Within this range of power especially interesting are radial-axial turbines. They have a very simple construction of the flow path and consist of only one or two symmetrical stages, which is expected to considerable reduce the costs of their production.

Literature

1. Duvia A., Gaia M., 2002, ORC plants for power production from biomasss from 0.4 to 1.5 MWe, Technology, efficiency, practical experiences and economy, Proc. 7th Holzenergie Symposium, ETH Zürich.
2. Щегляев А.В., 1976, Паровые турбины, М.: Энергия.
3. Русанов А.В., Пащенко Н.В., Косьянова А.И., 2009, Метод аналитического профилирования лопаточных венцов проточных частей осевых турбин, Восточно-Европейский журнал передовых технологий, Вып. 2/7 (38), 32–37.
4. Русанов А.В., Шатравка О.И. , Косьянова А.И., 2009, Профилирование радиально-осевых турбин с использованием современных компьютерных технологий, Восточно-Европейский журнал передовых технологий, Вып. 4/4 (40), 58–62.
5. Єршов С.В., Русанов А.В., 1996, Свідоцтво про державну реєстрацію прав автора на твір, ПА № 77. Державне агентство України з авторських та суміжних прав. Комплекс програм розрахунку тривимірних течій газу в багатовінцевих турбомашинах “FlowER” – 19.02.1996.
6. Русанов А.В., Єршов С.В., 2008, Математическое моделирование нестационар-ных газодинамических процессов в проточных частях турбомашин, Х.: ИПМаш НАНУ.
7. Lampart P., Rusanov A. , Yershov S., Marcinkowski S., Gardzilewicz A., 2005, Validation of 3D RANS Solver With a State Equation of Thermally Perfect and Calorically Imperfect Gas on a Multi-Stage Low-Pressure Steam Turbine Flow, Trans ASME Journal of Fluids Engineering, Vol. 127, 83–93.
8. Lampart P., Yershov S., Rusanov A., 2005, Increasing flow efficiency of high-pressure and low-pressure stream turbine stages from numerical optimization of 3D blading, Engineering Optimization, Vol. 37, 145–166.

Acknowledgment

The work was partly supported by the (Polish) National Centre for Research and Development (NCBiR): “Advanced Technologies for Energy Generation. Task 4: Elaboration of Integrated Technologies for the Production of Fuels and Energy from Biomass, Agricultural Waste and other Waste Materials”.

D. Sc. RUSANOV Andrey, Institute of Mechanical Engineering Problems, National Academy of Sciences of Ukraine, Department of Hydroaeromechanics, 2/10 Pozharskogo Str., Kharkov, Ukraine 61046, +38(057)752-33-88, rusanov@ipmach.kharkov.ua;

D. Sc. LAMPART Piotr, Institute of Fluid Flow Machinery, Polish Academy of Sciences, Department of Turbine Aerodynamics, Fiszera 14, 80-231 Gdańsk, Poland, +48 58 69 95 266, lampart@imp.gda.pl;

M. Sc. RUSANOV Roman, Institute of Mechanical Engineering Problems, National Academy of Sciences of Ukraine, Department of Hydroaeromechanics, 2/10 Pozharskogo Str., Kharkov, Ukraine 61046, +38(057)349-48-01, roman_rusanov@ipmach.kharkov.ua;

M.Sc. BYKUC Sebastian, Institute of Fluid Flow Machinery, Polish Academy of Sciences, Department of Turbine Aerodynamics, Fiszera 14, 80-231 Gdańsk, Poland, +48 58 69 95 144, sbykuc@imp.gda.pl.